

# The polarised gluon density $\Delta G$ from di-jet events in NLO

G. Rädcl<sup>a</sup> and A. De Roeck<sup>b</sup>

<sup>a</sup> DAPNIA/SPP, CEA Saclay, F-91191 Gif-sur-Yvette, France

<sup>b</sup> Deutsches Elektronen-Synchrotron DESY, Notkestrasse 85, D-22603 Hamburg, FRG

**Abstract:** A feasibility study to extract the polarised gluon density from di-jet events at HERA in next-to-leading order is presented. It is shown that when taking next-to-leading order effects into account the asymmetries at HERA remain measurable and sensitive to the polarised gluon distribution. They can be used to extract the polarised gluon density in the proton in the region  $0.005 < x_g < 0.4$ .

## 1 Introduction

The origin of the spin in the proton is still a subject of much debate. Over the years it has been confirmed that the quarks, as measured in deep inelastic scattering, account for only 30% of the proton spin. Next-to-leading order (NLO) QCD fits of structure function and semi-inclusive data suggest that the contribution of the gluon to the spin could be large [1, 2]. A first attempt of a direct measurement of the polarised gluon distribution,  $\Delta G$ , using leading charged particles [3] is not in conflict with this suggestion. In general, it has been concluded that major progress in our understanding of the spin structure can be made with clear and unambiguous direct measurements of  $\Delta G$ . Several experiments are planned to tackle this measurement [4, 5].

It has been shown that the  $ep$  collider HERA, when both beams are polarised, could make an important contribution to the determination of  $\Delta G(x)$ , for a considerable  $x$ -range, where  $x$  is the momentum fraction of the proton carried by the gluon. A particularly sensitive method is to extract  $\Delta G(x)$  from di-jet events in deep inelastic scattering. Feasibility studies of extracting the polarised gluon density  $\Delta G(x)$  from di-jet events at HERA in leading order (LO) have been performed [6, 7, 8, 9], the most detailed one was published in the proceedings of the workshop 'Future Physics with polarized beams at HERA' [8]. The event generator PEPSI [10], which includes hadronization of the final parton state, was used, followed by a simple detector simulation. PEPSI includes LO matrix elements for the QCD processes in the hadronic final state. A first estimate of higher order effects was obtained by including initial and final state *unpolarised* parton showers.

Recently next-to-leading order polarised cross sections for di-jet production became available with the program MEPJET [11, 12]. This allows to check NLO corrections to the LO cross section asymmetries. In this paper MEPJET will be used to find optimal event and di-jet

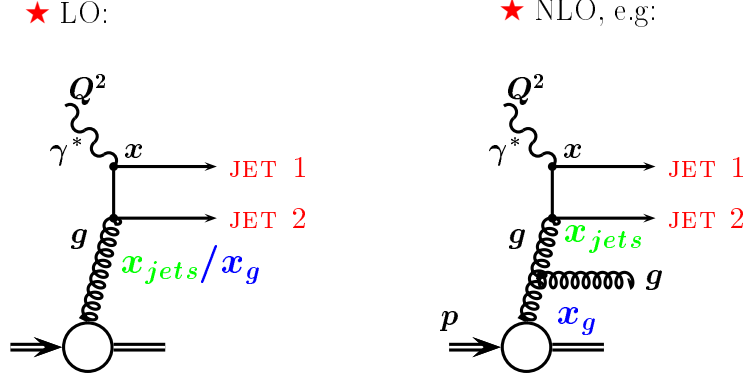


Figure 1: Feynman diagrams for the process of Boson-Gluon-Fusion (BGF) in LO (left) and a higher order process (right).

selection cuts, which are a balance between statistical significance and analysing power of the asymmetries.

Note that at LO the momentum fraction of the proton carried by the gluon,  $x_g$ , can be directly calculated from the di-jet kinematics (see Fig. 1). We define

$$x_{jets} = x(1 + \frac{\hat{s}}{Q^2}),$$

calculated from the Bjorken- $x$ , the four momentum transfer  $Q^2$  and the invariant mass  $\hat{s}$  of the di-jet system. At LO the variable  $x_{jets}$  is identical to  $x_g$ , while at NLO  $x_{jets}$  is different from  $x_g$  even at parton level e.g. due to gluon radiation processes, see Fig. 1. In fact the relation  $x_g \geq x_{jets}$  holds.

Since the main purpose of this paper is to show the size of the asymmetries in NLO and the range in  $x_g$  where one can expect information on  $\Delta G$ , a simple method to relate the reconstructed  $x_{jets}$  variable from the jets to the true one will be used. The same technique to unfold the gluon from the data as done at LO [8] will be used.

In the last chapter we show the potential of a future high energy  $ep$  collider, to extract  $\Delta G$  in LO from di-jet events, using TESLA and HERA as an example.

## 2 Di-jet selection using MEPJET

We start with kinematic cuts close to the ones used in the published LO study [8, 9]:

$$5 < Q^2 < 100 \text{ GeV}^2 \quad (1)$$

$$y > 0.3 \quad (2)$$

$$E_{electron} > 5 \text{ GeV} \quad (3)$$

$$p_t^{jets} > 5 \text{ GeV} \quad (4)$$

change to cuts (eqn. 1-4)					cross sections [pb]				$\frac{\Delta\sigma}{\sqrt{\sigma}} \sim \frac{A}{\delta A}$	
$\hat{s}$	$Q^2$	$y$	$p_t^{jets}$	$E_e$	LO		NLO			
[GeV <sup>2</sup> ]			[GeV]		unpol.	pol.	unpol.	pol.	LO	NLO
100					$1267 \pm 4$	$-44 \pm 0.1$	$1377 \pm 68$	$-24 \pm 2$	1.24	0.65
500					$378 \pm 2$	$-21 \pm 0.1$	$644 \pm 57$	$-20 \pm 2$	1.08	0.79
500	10				$293 \pm 2$	$-16 \pm 0.1$	$432 \pm 20$	$-12 \pm 1$	0.93	0.58
100	10				$920 \pm 3$	$-29 \pm 0.1$	$944 \pm 40$	$-16 \pm 2$	0.96	0.52
500	2				$407 \pm 2$	$-23 \pm 0.1$	$688 \pm 27$	$-16 \pm 2$	1.14	0.61
500		0.15			$526 \pm 3$	$-26 \pm 0.1$	$950 \pm 39$	$-20 \pm 1$	1.13	0.65
500	40				$104 \pm 1$		$130 \pm 10$			
200					$976 \pm 4$	$-36 \pm 0.1$	$1205 \pm 36$	$-23 \pm 1$	1.15	0.66
200			7		$497 \pm 2$	$-21 \pm 0.1$	$630 \pm 38$	$-18 \pm 1$	0.94	0.72
200			7	3	$539 \pm 3$	$-24 \pm 0.1$	$670 \pm 21$	$-18 \pm 1$	1.03	0.70
300					$674 \pm 3$	$-30 \pm 0.1$	$943 \pm 28$	$-21 \pm 1$	1.16	0.68
300				3	$730 \pm 3$	$-33 \pm 0.2$	$957 \pm 30$	$-21 \pm 2$	1.33	0.68

Table 1: Unpolarised and polarised di-jet cross-sections for different kinematic cuts, in LO and NLO. The cuts are the lower limits. The last two columns contain a measure for the analysing power (see text).

Compared to [8, 9], for the scattered electron and jet selection in this analysis, a pseudorapidity cut of  $|\eta| < 3.5$  is used. An additional cut on the  $p_t^{jets} > 5$  GeV in the Breit frame is also applied. As before the cone jet algorithm was used with a cone size of 1 in azimuthal angle and pseudorapidity. For the calculations we used the structure function parametrisations of GRV [13] for the unpolarised case, and Gehrmann-Stirling set A [14] for the polarised case. The cut on the square of the invariant mass of the two jets was varied in the range,  $\hat{s} := Q^2(x_{jets}/x - 1)$ , as

$$\hat{s} > 100, 200, 300, 500 \text{ GeV}^2,$$

where  $\hat{s}$  is computed from the reconstructed jet quantities, and the variables are indicated in Fig. 1. Further cuts which were varied in the study are:

$$p_t^{jets} > 5, 7 \text{ GeV},$$

$$Q^2 > 2, 5, 10, 40 \text{ GeV}^2,$$

$$y > 0.15, 0.3,$$

and finally the electron energy cut was lowered to  $E_e = 3 \text{ GeV}^2$ . The results for LO and NLO, polarised and unpolarised cross section for *exclusive* di-jet production for several combinations of cuts, can be seen in Table 1. In the last column of this table the ratio between the expected overall asymmetry ( $\Delta\sigma/\sigma$ ) and a quantity which is proportional to the expected statistical error ( $1/\sqrt{\sigma}$ ) has been computed, and hence gives an idea of the sensitivity: a higher value means higher sensitivity.

One observes that for all tried scenarios the sensitivity decreases from LO to NLO. Furthermore globally the corrections to the unpolarised cross sections become large for a high  $\hat{s}$  cut, while the polarised cross section receives high corrections when a low  $\hat{s}$  cut is used. For the final study we selected those scenarios where the correction to the polarised and unpolarised cross sections are less than 30% and a good compromise between the analysing power and statistics is found. This can be obtained by choosing  $\hat{s} > 300 \text{ GeV}^2$  or  $\hat{s} > 200 \text{ GeV}^2 \wedge p_t > 7 \text{ GeV}$ , both of which have a large sensitivity to the gluon according to Table 1. The asymmetries as a function of  $x_{jets}$  for these scenarios in LO and NLO are compared in Fig. 2. The values are reduced in NLO compared to LO, but still sufficiently large. The errors correspond to the statistical errors expected for  $200 \text{ pb}^{-1}$  (but assuming a 100% polarisation of the colliding beams). Table 1 also shows that lowering the electron energy requirement does not bring a significant improvement, despite the region of larger depolarisation factor included. We will therefore use the scenario of  $\hat{s} > 200 \text{ GeV}^2 \wedge p_t > 7 \text{ GeV}$  and  $E_e > 5 \text{ GeV}$  in the following.

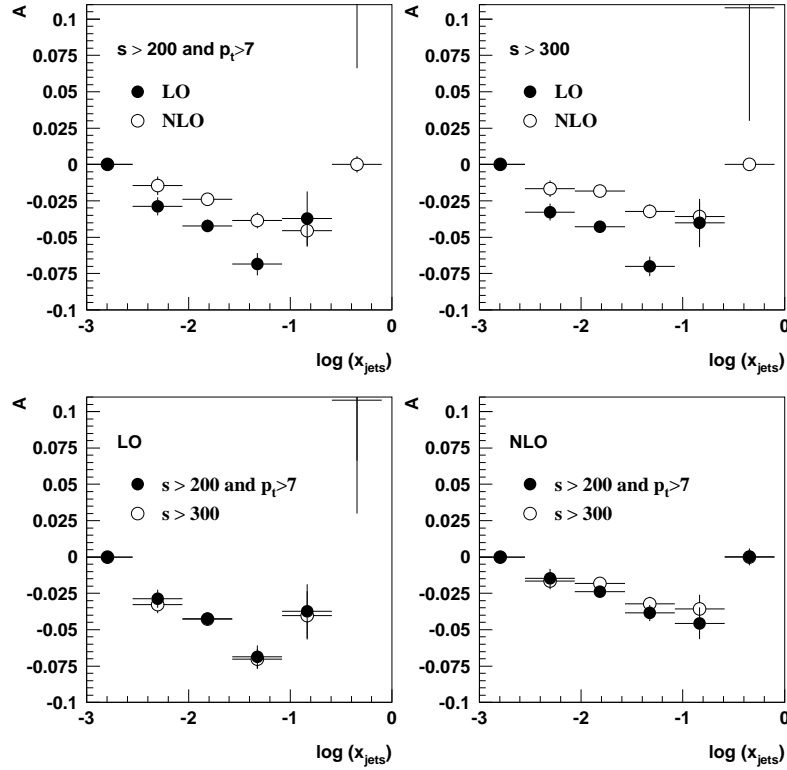


Figure 2: Comparison of the asymmetries versus  $x_{jets}$  in LO and NLO for the two selected cut scenarios (see text).

Before moving towards extracting the gluon distribution we first compare di-jet asymmetries in LO predicted by MEPJET with PEPSI without parton showers, and find them to agree very well. This has been shown before [8], and has been confirmed here. In Table 2 the overall asymmetries are shown using different  $\hat{s}$  cuts and event/jet selection cuts as in [8]. Using the standard cuts, as derived in this paper, i.e.  $\hat{s}_{min} > 200 \text{ GeV}$  and  $p_t^{jets} > 7 \text{ GeV}$ , the NLO and LO cross sections of MEPJET and PEPSI are compared in Table 3. For the higher order calculations, the largest difference is observed for the unpolarised cross sections (PEPSI/PS versus MEPJET/NLO) while the polarised cross sections are very similar.

	MEPJET	PEPSI
$\hat{s}_{min}$ [GeV]	A[%]	A [%]
100	$3.5 \pm 0.1$	$3.0 \pm 0.6$
200	$3.7 \pm 0.2$	$3.4 \pm 0.9$
500	$5.6 \pm 0.3$	$6.4 \pm 1.2$

Table 2: Asymmetries for MEPJET (LO) and PEPSI (no parton showers) for different values of the  $\hat{s}$  cut.

generator	mode	$\hat{\sigma}$ [pb]	$\Delta\sigma$ [pb]
MEPJET	LO	$539 \pm 3$	$-24 \pm 0.1$
MEPJET	NLO	$670 \pm 21$	$-18 \pm 1$
PEPSI	no PS	592	-27
PEPSI	PS	584	-20

Table 3: Asymmetries for MEPJET (LO/NLO) and PEPSI (with/without parton showers). The errors on the PEPSI results are of the order of 10%.

### 3 Correlation of 'true' and 'visible' variables

A problem of MEPJET is that the 'true'  $x_g$ , i.e. the  $x$  value of the gluon probed in the proton, is not known anymore at running time, but only the  $x$  value reconstructed from the mass of the two jets  $s_{ij} : x_{jets}$ . In contrast to the LO case, in NLO the information of the di-jets alone is not sufficient to reconstruct directly  $x_g$  event by event, but needs to be 'unfolded'. To be sensitive to  $\Delta G$  by measuring di-jet asymmetries only there has to be a good correlation between  $x_g$  and  $x_{jets}$ . This correlation has been checked using the program DISENT [15]. A correlation matrix has been produced, which in a second step can be used in MEPJET to reconstruct  $x_g$  from  $x_{jets}$ . DISENT contains only unpolarised di-jet cross sections therefore we could not perform the whole study with this program. For the simulation we used the same conditions as in MEPJET, concerning jet algorithm, parton distributions and cuts.

Fig. 3 (right) shows the correlation between  $x_g$  on the  $x$  axis and  $x_{jets}$  on  $y$ -axis. The correlation looks promising. This correlation matrix was then applied in the MEPJET program: for each 'event' the  $x_g$  was determined from the  $x_{jets}$  randomly according to the probabilities of this matrix. Fig. 3 (left) shows the polarised cross sections for gluon induced processes as a function of  $x_{jets}$  and the so-determined  $x_g$ . We see a shift to higher  $x$  as expected, but the corrections are not very large.

Figure 4 shows that also in NLO the polarised cross-section for di-jet production is dominated by gluon initiated processes. The corresponding asymmetries for events due to quark and gluon initiated processes, which can not be distinguished on an event by event basis, are shown in Fig. 5 for a luminosity of  $200 \text{ pb}^{-1}$ . The figure also shows the asymmetries when calculated versus the 'measured'  $x$  ( $x_{jets}$ ) or the 'true'  $x$  ( $x_{true} \equiv x_g$ ) when using the unfolding matrix from DISENT. It demonstrates that the effects are small due to the locality of the  $x_{jets} - x_g$  correlation.

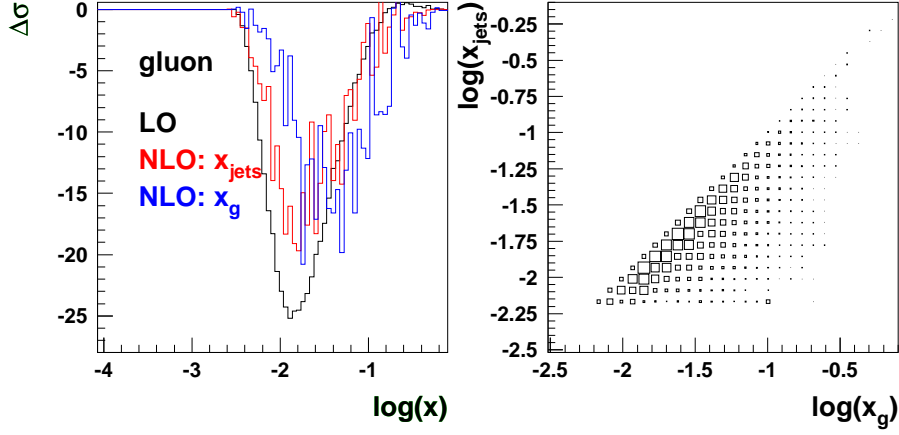


Figure 3: Left: the polarised cross section versus  $x$  (MEPJET) in LO and NLO. For the latter it is shown both as function of the  $x_g$  and  $x_{jets}$  using DISENT for the correction (see text). Right: the correlation between  $x_g$  and  $x_{jets}$  using the DISENT program.

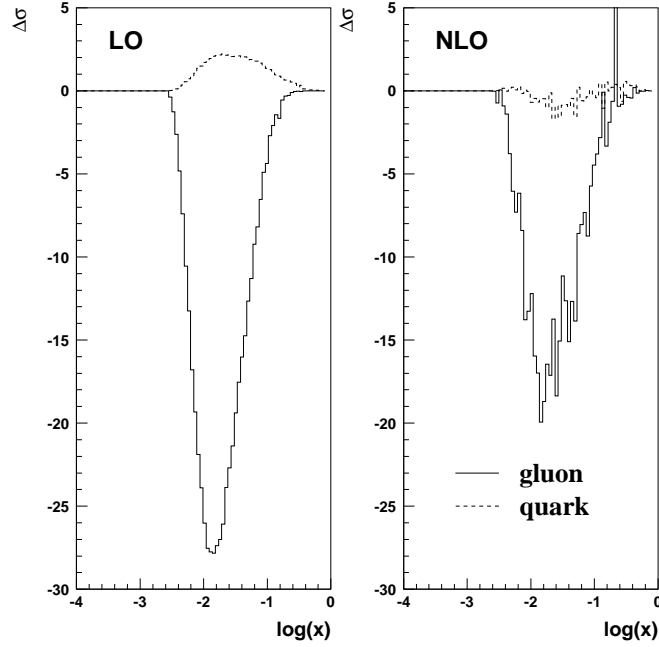


Figure 4: The polarised cross section versus  $x$  in LO (left) and NLO (right) for quark and gluon induced processes.

A comparison of the asymmetries expected in LO and in NLO, for the latter shown both as a function of  $x_g$  and  $x_{jets}$ , is given in Fig. 6. The reduction of the asymmetry from LO to NLO is clearly visible.

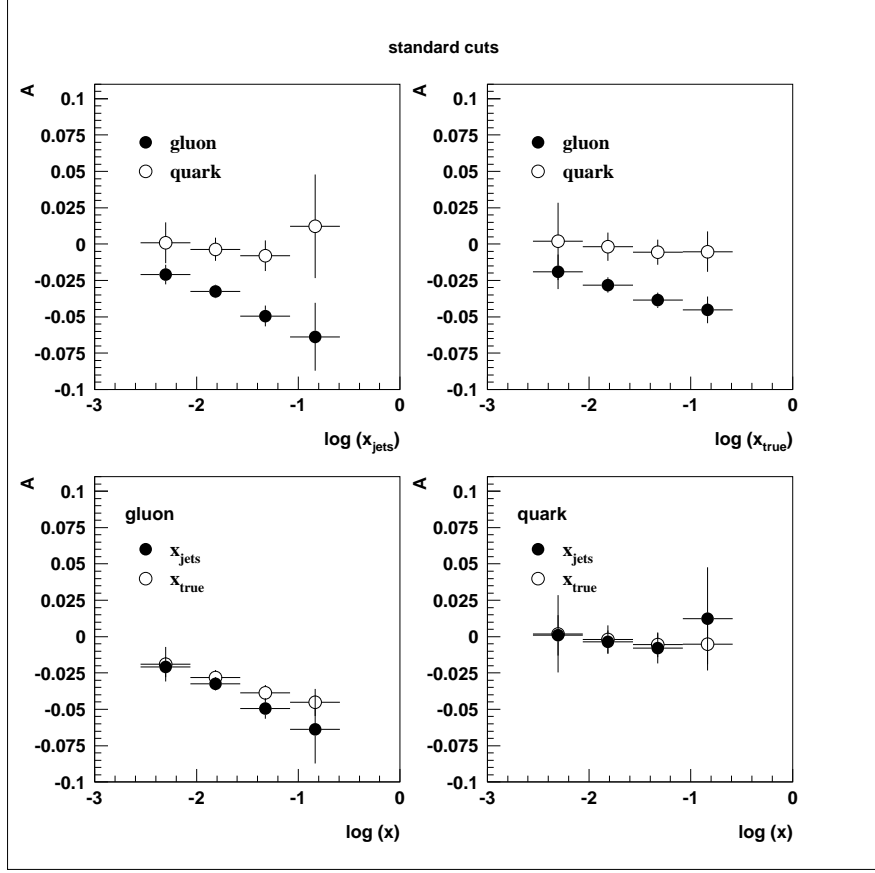


Figure 5: Top: the asymmetries for gluon and quark induced processes separately versus  $x_{jets}$  and  $x_g$ , labeled as  $x_{true}$  in the figure; Bottom: a direct comparison of the asymmetries versus  $x_{jets}$  and  $x_g$  for the gluon and quark induced processes separately.

## 4 Sensitivity to $x\Delta G(x)$

In this section we will quantify the sensitivity to the shape of  $x\Delta G(x)$ , following the method used in [8]. In a real measurement one could obtain  $x\Delta G(x)$  from the measured asymmetry by an unfolding method, where the background would be subtracted statistically and correlations between bins are fully taken into account. The H1 experiment has already shown a NLO extraction of the gluon by using combined information of the total inclusive and di-jet cross section [16]. If correlations between bins are small one can use a simpler method performing a bin-by-bin correction. For our study we consider the latter method to be sufficient.

Taking the NLO GS-A gluon distribution as a reference, we calculated the statistical errors of  $x\Delta G(x)$  in the range  $0.005 < x < 0.4$  where a significant measurement can be made. Note that this range is shifted slightly to higher  $x$  values compared to the LO study since  $x_g > x_{jets}$ . Also shown is the expectation for the NLO GS-C distribution. The results are shown for two values of the integrated luminosity and taking the polarisation for both beams to be 0.7. Clearly, even for a luminosity of only  $200 \text{ pb}^{-1}$  already a clear difference between the two gluon scenarios is expected.

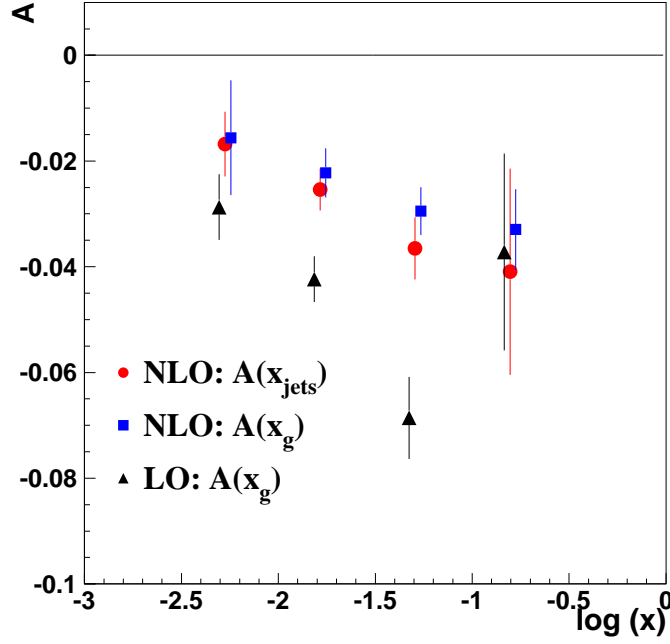


Figure 6: Comparison of the asymmetries in LO and NLO for the 'true'  $x_g$  and 'measured'  $x_{jets}$ .

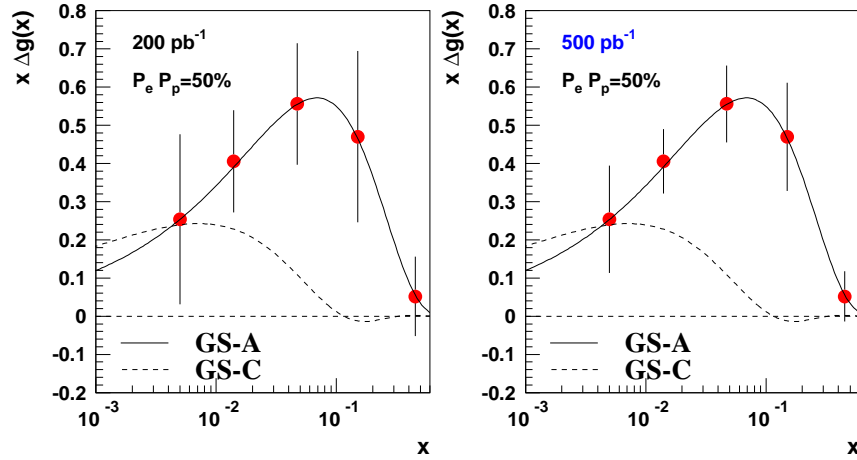


Figure 7: The statistical precision of a measurement of  $x\Delta G(x)$  from di-jets in NLO, shown on top of the GS-A parton density curve, for two values of integrated luminosity. The expected value for the beam polarisation is taken into account. GS-C is shown for reference.

## 5 HERA-TESLA

Finally the di-jet asymmetry was calculated for a possible future high energy  $ep$  collider, consisting on the one hand of the HERA proton ring, and on the other hand of a  $e^+e^-$  linear collider



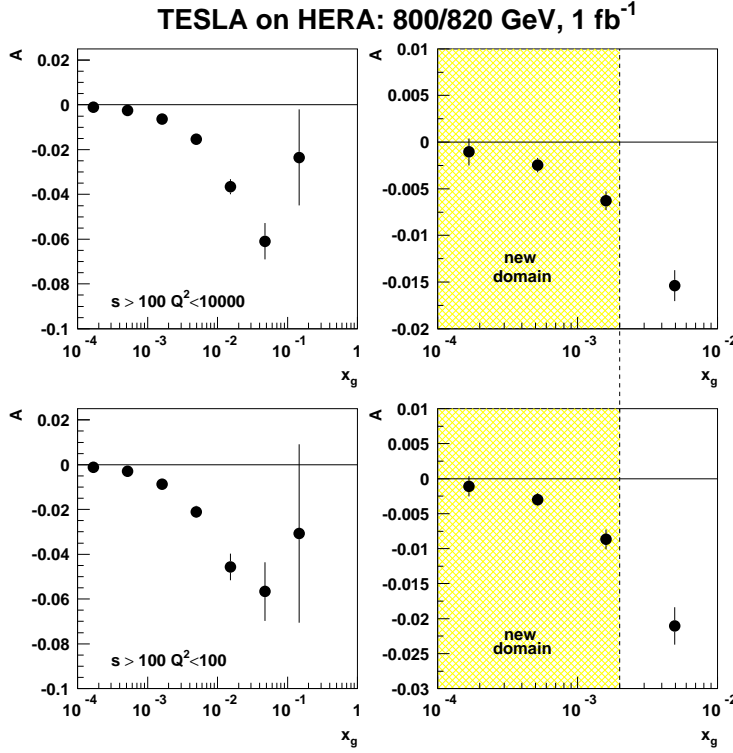


Figure 8: Asymmetries measured using a 800 GeV  $e^-$  beam of TESLA on a 820 GeV  $p$  beam of HERA, for two selected  $Q^2$  regions (top/bottom). On the left hand side the low  $x$  region is expanded and the newly reachable low- $x$  domain is shown by the hatched region of the plot.

(LC). DESY proceeds towards a proposal for such a linear collider, which would have a centre of mass system (CMS) energy of 0.5 – 1. TeV. It is planned to include the possibility to perform  $ep$  collisions, by constructing the LC tangential to HERA, allowing for an interaction region in the HERA West hall. The kinematics and beam dynamics have been discussed in [17, 18]. The polarisation of the electron beam would be sufficiently large (about 80%). If also the proton beam is polarised, polarised  $ep$  scattering can be studied at a CMS of about 1 TeV, allowing to study the polarised parton distributions at an order of magnitude lower in  $x$  compared to HERA. In [19] the gain for  $g_1$  is discussed. Here we show the asymmetries (in LO) for the di-jets, using the same jet selection criteria as used for the HERA study, for collisions of 820 GeV protons on 800 GeV electrons, possibly the maximum which can be expected. The error bars correspond to  $1000 \text{ pb}^{-1}$ , but the polarisation of the beams is assumed to be 100%. Events and jets are selected within the pseudorapidity range from  $-4$  to  $3.5$  for the jets and from  $-7$  to  $3.5$  for the scattered electron,  $Q^2 > 1 \text{ GeV}^2$ ,  $p_t^{jets} > 5 \text{ GeV}$ , and  $\hat{s} > 100 \text{ GeV}^2$ . The asymmetries are shown for two upper limits on  $Q^2$ . In the figures on the right the low- $x$  region is shown explicitly, and the gain in  $x$ -range with respect to nominal HERA is given by the shaded area. The measurement reflects the decreasing asymmetries with decreasing  $x$ . The asymmetries at very low  $x$  become very small. The lowest values of  $x$  where a significant measurement of the di-jet asymmetry can be made with TESLA-HERA will be about  $x = 0.0005$ . However a large statistics sample  $\mathcal{O}(1) \text{ fb}^{-1}$  and an excellent control of systematic errors will be needed.

## 6 Conclusion

The direct measurement of  $\Delta G(x)$  via di-jet production has been studied at NLO, using the MEPJET program. The asymmetries are reduced with respect to the LO case, but a sufficiently large sensitivity to the polarised gluon distribution can be obtained in the region  $0.005 < x_g < 0.4$  for luminosities larger than  $200 \text{ pb}^{-1}$ . This measurement can be extended by roughly an order of magnitude to lower  $x$  with future polarised  $ep$  collisions using TESLA and HERA.

## Acknowledgements

G.R. thanks Vernon Hughes and the U.S. Department of Energy for financial support.

## References

- [1] SMC, B. Adeva, Phys. Rev. **D58** (1998) 112002.
- [2] D. De Florian, O.A. Sampayo and R. Sassot, Phys. Rev. **D57** (1998) 5803.
- [3] HERMES collaboration, A. Airapetian et al., DESY-99-071 (1999).
- [4] COMPASS proposal, CERN/SPSLC/P297.
- [5] S. Heppelmann, proceedings of '12th Int. Symposium on High Energy Spin Physics', Amsterdam 1996, Eds. C.W. de Jager et al. (World Scientific, Singapore, 1997) 352.
- [6] J. Feltesse, F. Kunne, E. Mirkes, *Phys. Lett.* **B388** (1996) 832.
- [7] A. De Roeck *et al.*, hep-ph/9610315.
- [8] G. Rädcl, A. De Roeck and M. Maul, hep-ph/9711373.
- [9] A. De Roeck *et al.*, Eur. Phys. J. **C6** (1999) 121 hep-ph/9801300.
- [10] L. Mankiewicz, A. Schäfer, M. Veltri, *Comp. Phys. Comm.* **71** (1992) 305.  
O. Martin, M. Maul and A. Schäfer, hep-ph-971038.
- [11] E. Mirkes, D. Zeppenfeld, *Phys. Lett.* **B380** (1996) 205.
- [12] E. Mirkes and S. Willfarth, hep-ph/9711434.
- [13] M. Glück, E. Reya, A. Vogt, *Z. Phys.* **C67** (1995) 443.
- [14] T. Gehrmann, W.J. Stirling, *Phys. Rev.* **D53** (1996) 6100.
- [15] S. Catani and M. H. Seymour, *Acta Phys. Polon.* **B28** (1997) 863.
- [16] H1 Collaboration, Contributed paper to the ICHEP98, Vancouver, paper 520 (1998).
- [17] A. De Roeck, Turkish Journal of Physics, **22**, (1998) 595.
- [18] R. Brinkmann, Turkish Journal of Physics, **22**, (1998) 661.
- [19] A. Deshpande, these proceedings.